Morphology and Electrical Properties of Carbon-Black-Filled Poly(ϵ-caprolactone)/Poly(vinyl butyral) Nanocomposites

Tzong-Ming Wu, Jen-Chih Cheng

Department of Material Science and Engineering, National Chung Hsing University, 250 Kuo-Kuang Road, Taichung 402, Taiwan, Republic of China

Received 7 January 2002; accepted 15 April 2002

ABSTRACT: The morphology of poly(ε-caprolactone) (PCL)/poly(vinyl butyral) (PVB)/clay nanocomposites was studied as a function of a small amount of amorphous PVB by polarized optical microscopy. The band spacings of PCL spherulites in PCL/PVB/clay nanocomposites decreased with increasing PVB content, and this indicated that increasing the PVB content shortened the period of lamellar twisting. The electrical properties of PCL/PVB/clay nanocomposites containing carbon black (CB) were also measured as a function of the PVB content. For samples with the same CB content, the intensity of the positive temperature coefficient (defined as the ratio of the peak resistivity to the resistivity at room temperature) of the nanocomposites increased as the PVB content increased. The change in the positive temperature coefficient was related to the morphological differences (i.e., the period of lamellar twisting) in the nanocomposites. © 2003 Wiley Periodicals, Inc. J Appl Polym Sci 88: 1022–1031, 2003

Key words: nanocomposites; morphology; spherulite

INTRODUCTION

The ability of polymers to act as electrical insulators is the basis for their wide use in the fields of electricity and electronics. However, material designers have sought to combine the fabrication versatility of polymers with many of the electrical properties of metals. When increased conductivity or permittivity of polymers is warranted, they can be used for low-temperature heaters, electromagnetic radiation shielding, antistatic materials, and electrical field grading. The method most often used to increase the electrical conductivity of insulating polymeric materials is combination with a conductive filler, such as carbon black (CB), carbon fiber, graphite, or metal foil, throughout the polymer matrix. Because of the ease of fabrication and low cost, the utilization of conductive CB-filled polymers has been significant. The conductivity of CB-filled polymers depends not only on the properties of CB, such as the particle size, aggregate shape, concentration, and dispersion state, but also on the characteristics of the polymers, such as the chemical structure, crystallinity, and processing conditions.[1–10] A crystalline polymer filled with a critical amount of CB shows a sharp electrical resistance increase with the temperature around the melting temperature of the polymer, and this is called the *positive temperature coefficient* (PTC). Important industrial applications of PTC materials are self-regulating heaters, current protection devices, microswitches, sensors, and electromagnetic interference shields.

The PTC phenomenon has attracted much interest over the past 2 decades.[11–15] Although there is no satisfactory theory explaining the PTC phenomenon, there have been many models elucidating its specific aspects, such as thermal expansion,[11] electron tunneling,[12–13] thermal fluctuation-induced tunneling,[14] double percolation,[9,15–18] and the cooperative effect of changes in the crystallinity and volume expansion.[7] At present, the explanation based on the tunneling effect is widely accepted. According to this mechanism, electrons pass through the thin gaps between adjacent CB particles, aggregates, and agglomerates at a practical magnitude of the electrical field. However, the effect of the blend morphology on the electrical conductivity of CB-filled polymer blends is based on the percolation theory.[15–18] The critical amount of CB necessary to build up a continuous conductive network is called the *percolation threshold*. In this case, CB particles are localized either in the continuous phase of only one polymer or at the interface of the cocontinuous phase of two polymers. Therefore, the conductivity of polymer blends is greatly influenced by the morphology of the polymer blends. From this point of view, there is a very interesting polymer blend system, poly(ε-caprolactone) (PCL)/poly(vinyl butyral) (PVB), reported by Keith et al.,[19] in which the nucleation frequency of the PCL crystals was strikingly reduced by the blending

Correspondence to: T.-M. Wu (tmwu@dragon.nchu.edu.tw).
Contract grant sponsor: National Science Council (NSC); contract grant number: NSC90-2216-E-005-026.

of only up to several percent of amorphous PVB. The addition of only 1% PVB dramatically reduced the nucleation density and allowed the spherulites of PCL to grow on the order of centimeters. The morphological changes included a marked enhancement in the regularity of the lamellar organization in the banded spherulites. Therefore, PCL/PVB blends are suitable for studying the effect of morphological changes on PTC properties because of the remarkable changes in the morphology of PCL/PVB and the dimensions of the spherulites of the blends (ca. 10 mm).[20,21]

Polymer nanocomposites, in which a polymer component is dispersed on a nanometer scale, have been attracting interest as a new field of research because of their excellent thermal, mechanical, transparency, and anticombustion properties.[22–25] The preparation of synthesized polymer nanocomposites involves the intercalation of monomers or polymers into swellable layered silicate hosts. In most cases, the synthesis involves either intercalation of a suitable monomer and then exfoliation of the layered host into their nanoscale elements by subsequent polymerization or melt-direct polymer intercalation with a conventional polymer extrusion process. The high aspect ratio of layered silicate can affect the physical and mechanical properties of the synthesized polymer nanocomposites. In this study, polymer nanocomposites containing polymer blends and CB were used to prepare conductive-filler-filled polymer nanocomposites. The morphology of these polymer nanocomposites containing crystalline/amorphous polymer blends with no ingredients was developed, and it was greatly influenced by the miscibility of the polymer blends. However, there has been no extensive investigation into the crystallization and morphology of the polymer nanocomposites containing conductive fillers, especially CB. The difficulty of this investigation is attributable to the fact that the presence of CB could hinder microscopic observations during the crystallization process.

In this report, we used swellable layered montmorillonite interacting with CB as the dispersed phase to prepare conductive-filler-filled PCL/PVB/clay nanocomposites. The effect of nanoscale montmorillonite on the morphology and electrical properties of PCL/PVB polymer nanocomposites was investigated.

EXPERIMENTAL

Specimens

The PCL and PVB used in this study were purchased from Polysciences, Inc. (Warrington, PA). The weight-average molecular weights of PCL and PVB were 35,000 and 100,000, respectively. Natural sodium montmorillonite with a trioctahedral smectite structure and a cation-exchange capacity of 110 mequiv/100 g was used as the dispersed phase to improve the distribution of CB. The surface of the natural sodium montmorillonite was treated with *n*-hexadecyl trimethyl-ammonium bromide and then mixed with a solution of CB. The 1 wt % treated clay with CB was then added to a PCL/PVB solution; this was mixed for 2 h and dried in a vacuum oven at 45°C for 2 h.

Wide-angle X-ray diffraction

X-ray $\theta/2\theta$ diffraction scans of these specimens were obtained with a 3-kW Rigaku III diffractometer (The Woodlands, TX) equipped with Ni-filtered Cu Kα radiation. These data were recorded in the reflection mode. The degree of crystallinity of THE PCL/PVB/clay nanocomposites was calculated from the integrated area of X-ray diffraction data, for which we assumed Gaussian profiles for crystalline and amorphous peaks.

Thermal analysis

The thermal analysis of the samples was performed with a PerkinElmer DSC7 differential scanning calorimeter (Norwalk, CT) calibrated with indium, and all experiments were carried out under a nitrogen atmosphere.

Polarized optical microscopy (POM)

Optical microscopy was performed with a Zeiss (Chester, VA) optical microscope equipped with a Mettler FP-82 (Columbus, OH) hot stage and crossed polarizers. The crystallization process was examined with the following temperature sequence. The polymer was heated to melting at 80°C for 20 min on the hot stage for the removal of the previous thermal history and then cooled quickly to 41°C for isothermal crystallization. Optical microscopy was recorded at 41°C for various times.

Electrical properties

Film samples of the nanocomposites were cast onto the surfaces of glass plates, and then silver paste was painted on both ends of the surfaces so that electrical contact with the electrodes would be ensured. The species were treated at 45°C for 30 min and then cooled in air to room temperature. The thickness of the thin films was approximately 0.15 mm. The temperature–resistivity curves of the nanocomposites were measured by SM-823, and the samples were heated at a rate of 1°C/min to 70°C during the resistivity measurements. Each datum shown is the mean value of measurements from at least three samples.

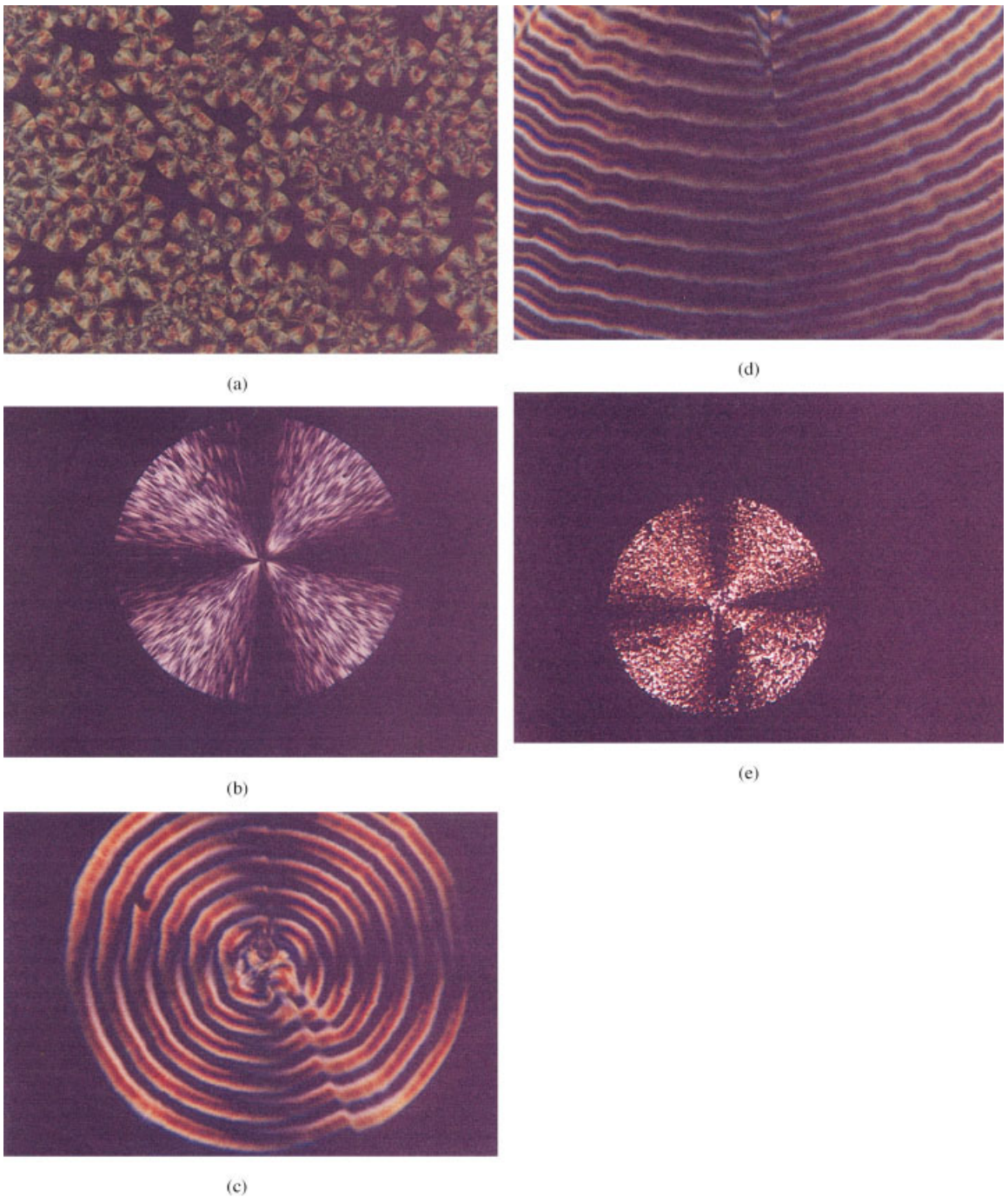

Figure 1 (a–d) Cross-polarized optical micrographs showing the extinction rings of various PCL/PVB spherulites without CB crystallized at 41°C and (e) cross-polarized optical micrograph of 5 wt % PVB in PCL/PVB with CB crystallized at 41°C.

RESULTS AND DISCUSSION

Figure 1(a–d) shows POM images of various PCL/PVB blends without CB crystallized at 41°C. When pure PCL was crystallized from the melt, the grown spherulites showed typical extinction crosses under polarizing microscopy. With the addition of 1 wt % amorphous PVB to PCL, larger spherulites could be observed because of the decreasing nucleation density in PCL with the presence of a small amount of PVB. With the addition of more PVB (up to 5–10 wt %), the specimens could be stored for at least 20 min at 41°C without nucleation occurring at all. The spherulites grown in PCL/PVB additionally exhibited banding with small radial separations of approximately 20 μm. This banding in the polymer spherulites was attributable to a twisting of the crystallographic orientation about the radii that apparently reflected cooperative twisting of radiating lamellar crystals about their axes of fastest growth. Its occurrence implied a high degree of coordination in the packing of the lamellae within a

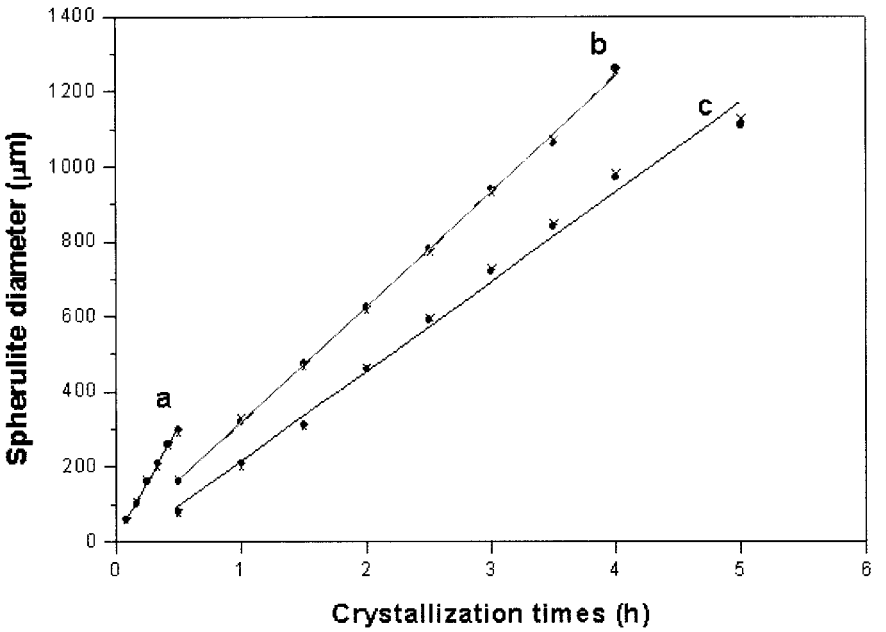

Figure 2 Spherulite diameter versus the crystallization time for PCL/PVB with (a) 1, (b) 5, and (c) 10 wt % PVB: (●) samples containing 5 wt % CB and (×) samples without CB. All the results are for crystallization at 41°C.

fairly compact structure. This result was remarkable for its potency in suppressing the primary nucleation of spherulites. Once nucleated, however, spherulites in PCL/PVB grew at radial rates comparable magnitude to those observed in undiluted PCL at the same temperature. The band spacings decreased with increasing PVB content, and this indicated that increasing the PVB content shortened the period of lamellar twisting. However, the spacings varied from place to place even in the same spherulite, and a quantitative comparison was impossible. Figure 1(e) shows the POM image of 5 wt % PVB in PCL/PVB with CB crystallized at 41°C. The presence of CB made it impossible to distinguish the growing boundaries of the spherulites from one another. Despite the poor visual field with CB in the melt and in the spherulite, larger spherulites with a Maltese cross in PCL/PVB were observed. The nucleation density in PCL/PVB with CB was similar to that observed for the system without CB. The growth front of the spherulite was also clearly observed with the presence of CB. These results of microscopic observations during crystal-

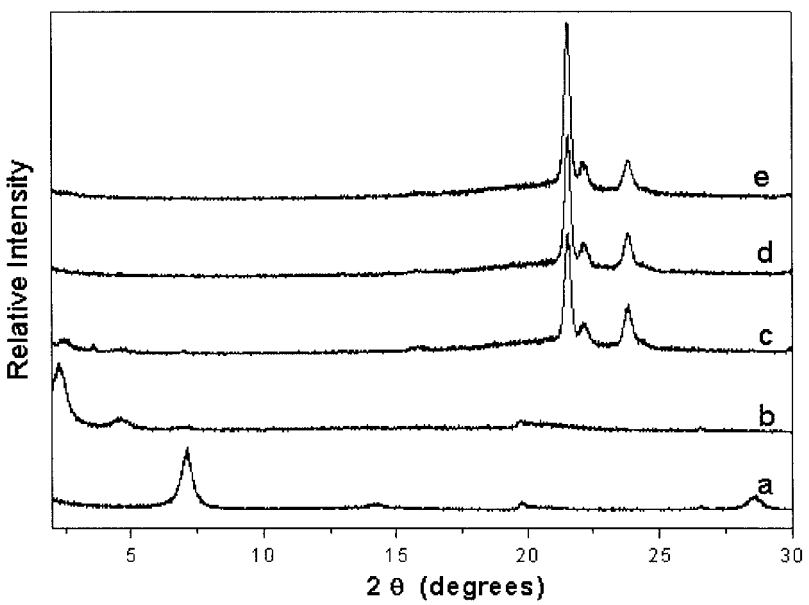

Figure 3 X-ray diffraction data for (a) neat layered montmorillonite, (b) the surface modification of montmorillonite, (c) PCL/clay, (d) 5 wt % PVB in PCL/PVB/clay nanocomposites, and (e) 5 wt % PVB in PCL/PVB/CB/clay nanocomposites.

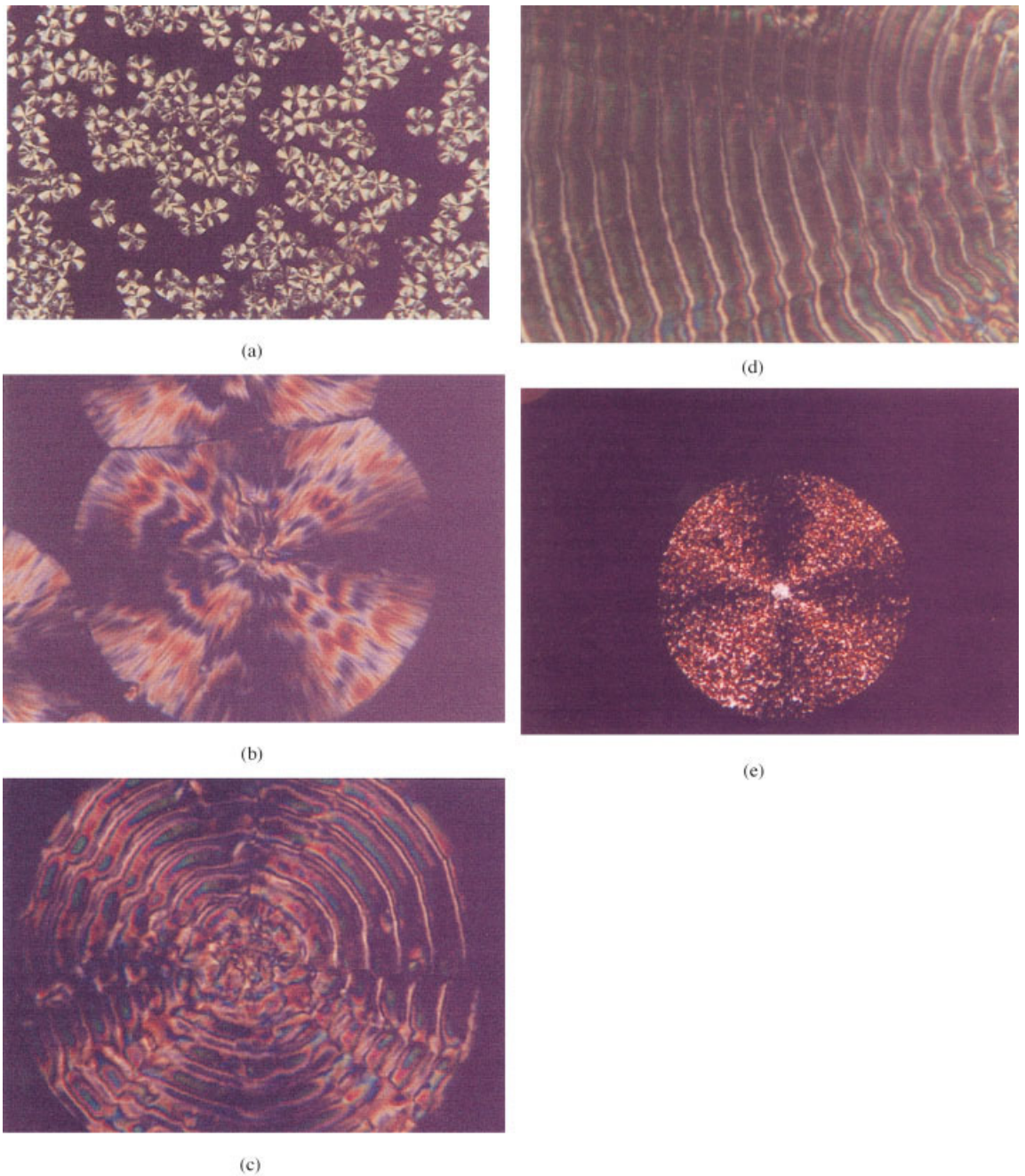

Figure 4 (a–d) Cross-polarized optical micrographs showing the extinction rings of various PCL/PVB/clay spherulites without CB crystallized at 41°C and (e) cross-polarized optical micrograph of 5 wt % PVB in PCL/PVB/clay with CB crystallized at 41°C.

lization were used to estimate the spherulite growth rate.

Figure 2 shows the dependence of the PVB content on the growth rate of the spherulites in PCL/PVB polymer blends with and without CB. An almost straight line was obtained for each sample, and the growth rate ($G = dR/dt$, where R is the radius of a spherulite) was determined from the slope of each line. The growth rate was lower for PCL/PVB than that for pure PCL and decreased with an increasing content of PVB but only to a degree (by a factor of ca. 1.5–2 at 41°C for 10 wt % PVB) that was not inordinate in comparison with what is commonly observed in polymers containing amorphous PVB. These observations showed that the crystallization of PCL/PVB was retarded by the addition of PVB, whereas CB had little effect on the nucleation of PCL or the spherulite growth rate.

According to these results, the growth rate should decrease during crystallization because of the increase in the diluent concentration at the growth front if an amorphous material is rejected by the growing lamel-

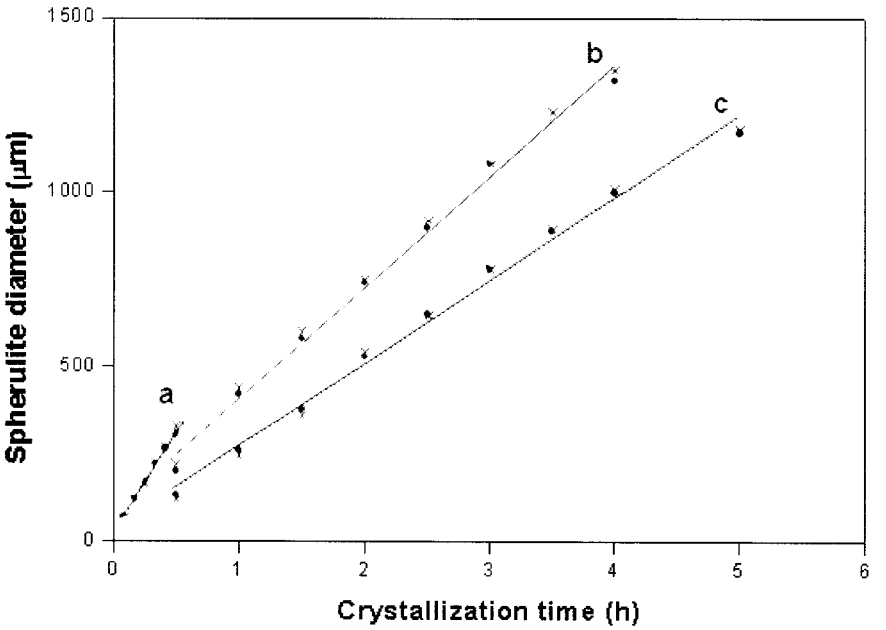

Figure 5 Spherulite diameter versus the crystallization time for PCL/PVB/clay with (a) 1, (b) 5, and (c) 10 wt % PVB: (●) samples containing 5 wt % CB and (×) samples without CB. All the results are for crystallization at 41°C.

lae. As the spherulites grow, the diluent concentration increases rapidly around the impinging spherulites. This causes a marked reduction in the growth rate and a flattening of the round spherulite profile. However, such flattening was not observed in this study. This implies that the concentration of the crystallizable component at the growing front remained constant throughout the spherulite growth. In the PCL/PVB system, a polar interaction between PCL and PVB prevented strong segregation of PVB. Therefore, PVB was not expelled from the spherulites and remained mainly in the amorphous layer between the PCL lamellae. Although these observations gave us a very important insight into the behavior of the blended polymers, we obtained no information on the distribution of CB in the spherulites because CB was too small to be observed by optical microscopy.

Figure 3 shows X-ray diffraction data of neat layered montmorillonite, organically modified montmorillonite, PCL/clay, and 5 wt % PVB in PCL/PVB/clay and PCL/PVB/clay/CB nanocomposites. The interlayer distances of the clays were obtained from the peak position (d_{001} reflection) of wide-angle X-ray diffraction traces. The d_{001} reflection for the neat layered montmorillonite was found at $2\theta \approx 7.14°$, which corresponded to an interlayer distance of 12.4 Å [Fig. 3(a)]. Organoclay modification shifted the X-ray data into smaller angles and substantially increased the interlayer distances. The reflection of organoclay [Fig. 3(b)] was found at $2\theta = 2.3°$, corresponding to an interlayer distance of 38.4 Å. Therefore, modified layered montmorillonite could probably be used as the medium of dispersion for the intercalation of a conductive filler and a polymer matrix. The X-ray diffraction data [Fig. 3(c–e)] for the solution intercalation of PCL/PVB into organically modified montmorillonite with or without CB exhibited no d_{001} reflection in the relevant region, indicating the presence of interlayer distances larger than 4.8 nm and exfoliation and random dispersion of PCL/PVB into the swellable layered silicate with or without CB. Therefore, PCL/PVB/clay nanocomposites are probably suitable for studying the effect of morphological changes on the PTC properties due to the presence of possibly remarkable changes in the morphology of the PCL/PVB/clay blends like those observed for PCL/PVB blends.

Figure 4(a–d) shows the POM images of various PCL/PVB/clay blends without CB crystallized at 41°C. When PCL/clay was crystallized from the melt, the grown spherulites showed extinction crosses under POM similar to those observed for pure PCL. In the PCL/PVB/clay system, with the addition of clay to PCL/PVB, all POM data showed a decreasing nucleation density in PCL/PVB with the presence of a small amount of clay. The spherulites grown in PCL/PVB/clay also exhibited banding with small radial separations, but the band spacings decreased with increasing PVB content and the addition of clay; this indicated that increasing the PVB content and adding clay shortened the period of lamellar twisting. In general, the nucleation density and banding spacings of the PCL/PVB systems decreased with the addition of clay to PCL/PVB. Figure 4(e) shows the POM image of 5 wt % PVB in PCL/PVB/clay with CB crystallized at 41°C. The presence of CB in PCL/PVB/clay also made it impossible to distinguish the growing boundaries of the spherulites from one another. Larger spherulites

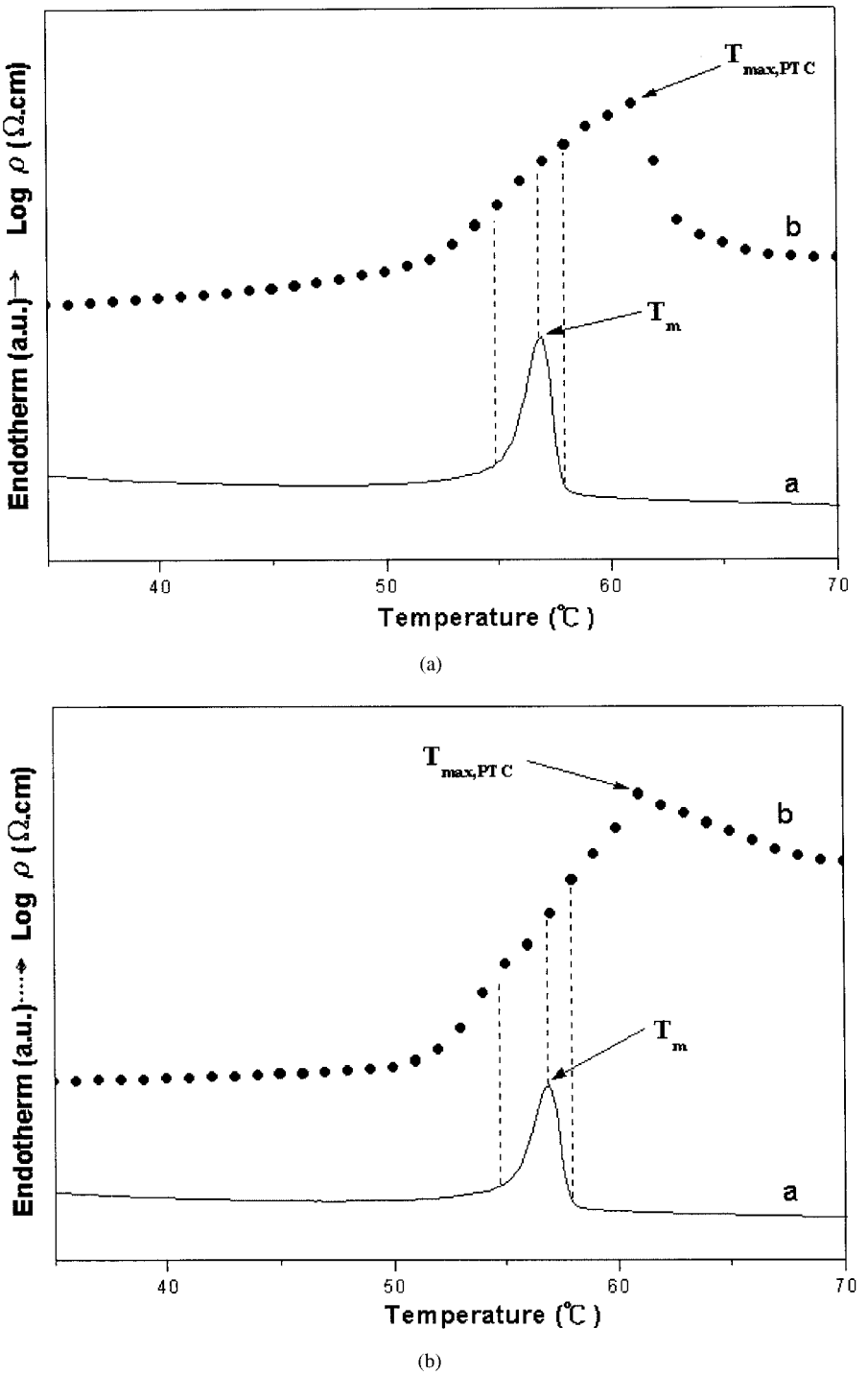

Figure 6 Temperature dependence of the resistivity (ρ) and the DSC melting curve of (a) pure PCL with 5 wt % CB and (b) 5 wt % PVB in PCL/PVB with 5 wt % CB.

with a Maltese cross in PCL/PVB/clay were observed despite the presence of a poor visual field with CB. The nucleation density in PCL/PVB/clay with CB was similar to that observed for the system without CB, and the growth front of the spherulite was clearly observed with the presence of CB. Therefore, the spherulite growth rate could be estimated from these microscopic observations during isothermal crystallization.

Figure 5 shows the PVB content dependence on the growth rate of the spherulites in PCL/PVB/clay polymer nanocomposites with and without CB. An almost straight line was obtained for each sample. The growth rates determined from the slope of each line were smaller in the PCL/PVB/clay than those in the PCL/clay and decreased with increasing contents of PVB. These observations showed that the crystallization of the PCL/PVB/clay was retarded by the addi-

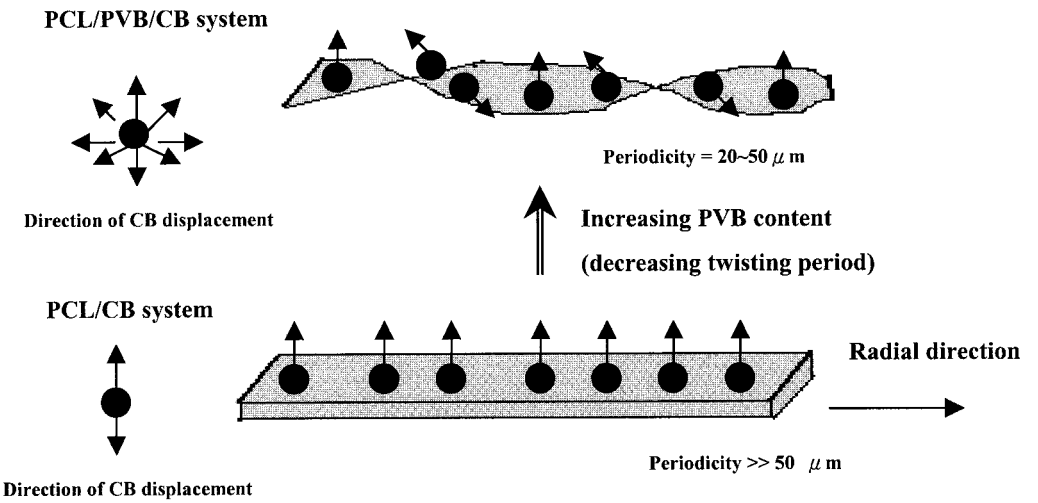

Figure 7 Schematic presentation of the CB distribution in PCL/PVB/CB systems.

tion of PVB, whereas CB had little effect on the nucleation of PCL/clay or the spherulite growth rate.

According to these results, the growth rate of PCL/PVB/clay decreased during crystallization with increasing PVB concentration and was similar to the growth rates observed for the PCL/PVB system. As the spherulites grew, the increasing amorphous PVB concentration did not cause a marked reduction in the growth rate and a flattening of the round spherulite profile. This implied that the concentration of the crystallizable PCL component at the growing front remained constant throughout the spherulite growth. In the PCL/PVB/clay nanocomposites, the addition of nanoscale clay had little effect on the nucleation of PCL or on the morphology of the spherulites. Therefore, PVB remained mainly in the amorphous layer between the PCL lamellae in the PCL/PVB/clay nanocomposites.

Figure 6 shows the temperature dependence of the resistivity and DSC melting curve of pure PCL with 5 wt % CB and 5 wt % PVB in PCL/PVB with 5 wt % CB. The resistivity–temperature curve slightly shifted upward with the presence of PVB, and the PTC intensity (I_{PTC}), defined as the resistivity ratio ρ_{max}/ρ_{min}, was also increased. Here ρ_{max} is the maximum value of the curve, and ρ_{min} is the resistivity at room temperature. The resistivity started to increase when the lamellar crystals began to melt and abruptly increased when the temperature approached $T_{max,DSC}$ (i.e., peak temperature measured by DSC). It reached a maximum around $T_{max,DSC}$ and started to decrease gradually after that temperature as a result of the reagglomerization of CB particles in the molten polymer phase (negative temperature coefficient). Therefore, the resistivity change was strongly related to the melting process. These results indicated that the drastic PTC property change originated from the abrupt volume expansion of melting lamellae that displaced CB. Therefore, it changed the distribution of interparticle gaps and the resistivity of PTC materials. Figure 7 shows a schematic presentation of the situation, with a conductive path lying along the crystalline lamellae or fibril in the spherulite. When the PCL crystalline lamellae melted, they changed the interparticle gap width and made the distribution more random. Most of the CB particles in the PCL/PVB/clay system moved perpendicularly to the surface of nontwisted lamellae, whereas CB close to twisted lamellae moved in almost all directions. Increasing the PVB content reduced the period of the lamellar twist; this increased the displacement of CB near the lamellar surface.

Figure 8 shows the effect of the content of CB on the PTC properties with the same amount of PVB. I_{PTC} increased with the CB ratio up to 5 wt % and then gradually decreased with the CB ratio up to 10 wt %. At least three specimens for a given CB ratio were measured. We used 5% CB for the following PCL/PVB/clay preparation. Figure 9 shows the effect of the PVB ratio on the PTC properties of PCL/PVB/clay nanocomposites containing 5 wt % CB. With the addition of as little as 2 wt % PVB, I_{PTC} increased more than 5 times with respect to that of PCL/clay. Surprisingly, I_{PTC} of the nanocomposites with 5 wt % PVB was larger than that of PCL/clay by almost 15 orders of magnitude. The amount of these nanocomposites was the same as the amount of CB, and the difference was only in the PVB concentration. Additionally, to verify the fact that drastic changes in the PTC properties did not come from the changes in the crystalline properties of PCL, we measured the crystallinity of the materials. Figure 10 shows the X-ray data for various PVB contents in PCL/PVB/clay nanocomposites with 5 wt % CB. All the results showed a similar X-ray pattern, indicating that the addition of amorphous PVB to crystalline PCL in the presence of clay and CB did not significantly change the crystalline structure of

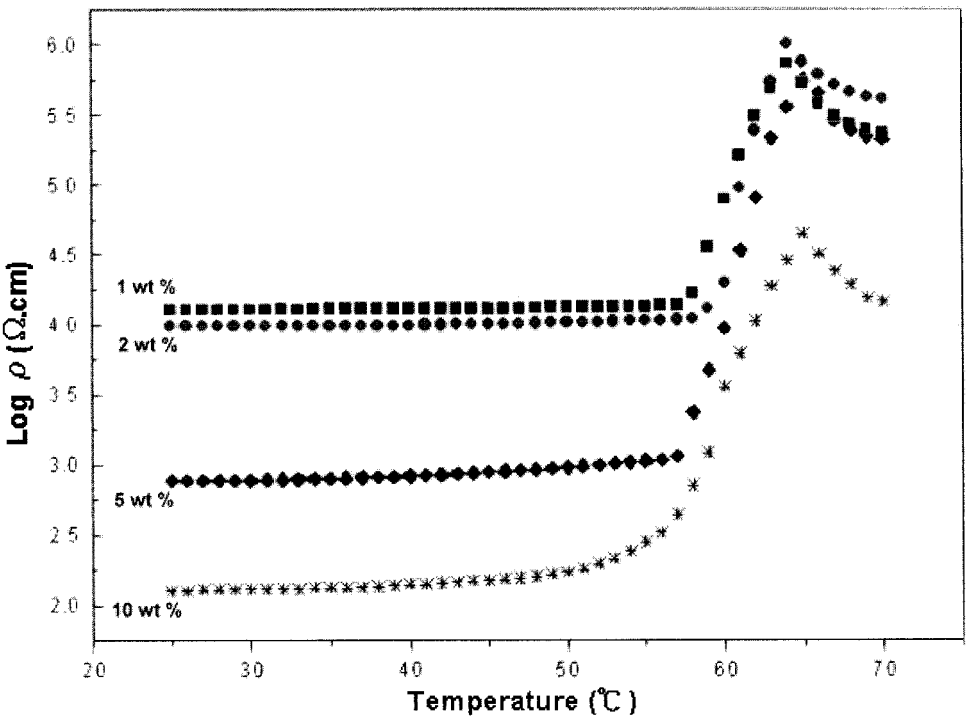

Figure 8 Effect of the content of CB on the PTC properties of PCL/PVB/clay nanocomposites.

PCL. The crystallinity of the specimens was obtained via curve fitting used to calculate the area of each peak. A linear background correction was applied separately to the observed peaks beforehand so that the area of each peak, for which we assumed Gaussian profiles, could be obtained. The calculated crystallinities for various PVB contents in PCL/PVB/clay nanocomposites showed no noticeable change for at least 10 wt % PVB.

According to these results, the increasing PVB concentration in the PCL/PVB/clay nanocomposites drastically reduced the band spacing, whereas I_{PTC} increased. The

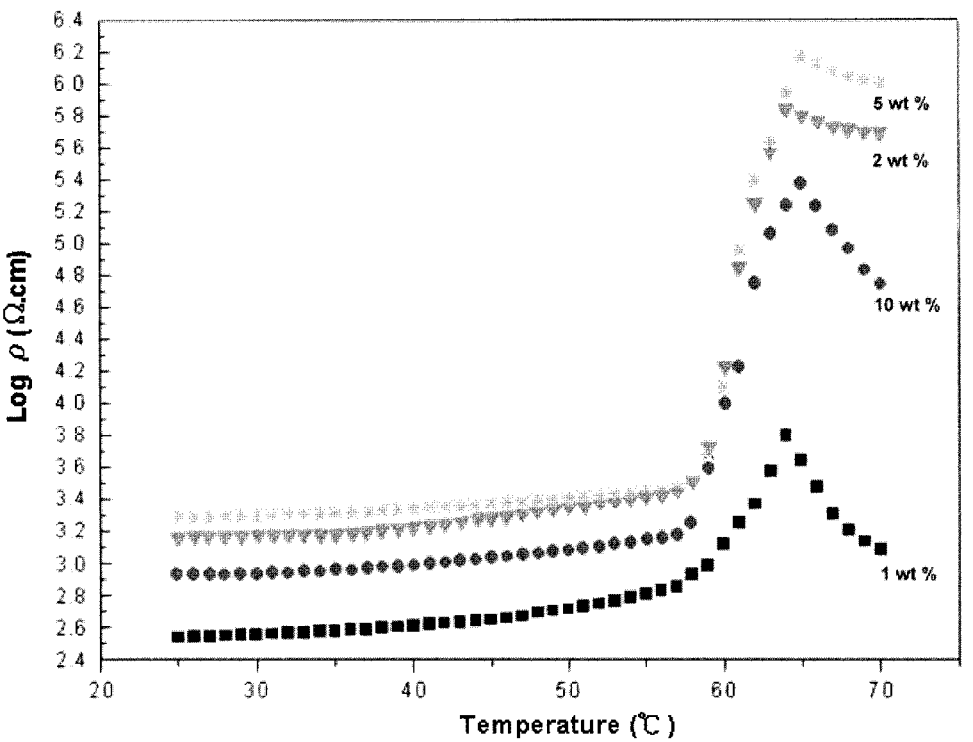

Figure 9 Effect of the PVB ratio on the PTC properties of PCL/PVB/clay nanocomposites containing 5 wt % CB.

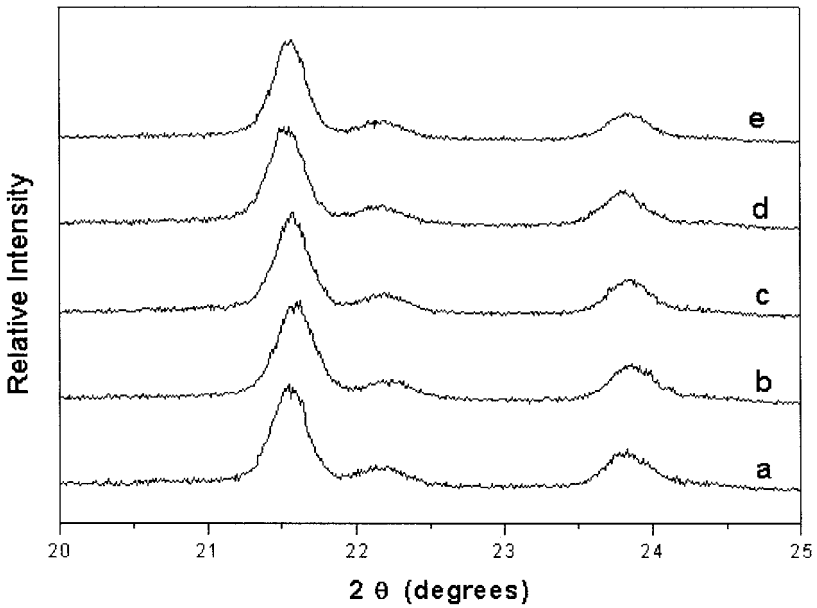

Figure 10 X-ray data for (a) pure PCL/clay and (b) 1, (c) 2, (d) 5, and (e) 10 wt % PVB in PCL/PVB/clay nanocomposites with 5 wt % CB.

influence of clay on I_{PTC} was less profound than that of the PVB concentration. These results indicated that increasing the PVB content shortened the period of lamellar twisting and caused a more complex displacement of CB in the melting process.

CONCLUSIONS

The band spacings of PCL spherulites in PCL/PVB/clay nanocomposites decreased with increasing PVB content, and this indicated that increasing the PVB content shortened the period of lamellar twisting. I_{PTC} of the nanocomposites increased as the PVB content increased. These results indicated that increasing the PVB content shortened the period of lamellar twisting and caused a more complex displacement of CB in the melting process.

References

1. Narkis, M.; Ram, A.; Flashner, F. Polym Eng Sci 1978, 18, 649.
2. Yu, G.; Zhang, M. Q.; Zeng, H. M. J Appl Polym Sci 1998, 70, 559.
3. Zhang, M. Q.; Yu, G.; Zeng, H. M.; Zhang, H. B.; Hou, Y. H. Macromolecules 1998, 31, 6724.
4. Yi, X.-S.; Wu, G.; Ma, D. J Appl Polym Sci 1998, 67, 131.
5. Knackstedt, M. A.; Roberts, A. P. Macromolecules 1996, 29, 1369.
6. Sumita, M.; Sakata, K.; Hayakawa, Y.; Asai, S.; Miyasaka, K.; Tanemura, M. Colloid Polym Sci 1992, 270, 134.
7. Al-Allak, H. M.; Brinkman, A. W.; Woods, J. J Mater Sci 1993, 28, 117.
8. Wang, B.; Yi, X.; Pan, Y.; Shan, H. J Mater Sci Lett 1997, 16, 2005.
9. Sumita, M.; Sakata, K.; Asai, S.; Miyasaka, K.; Nakagawa, H. Polym Bull 1991, 25, 265.
10. Gubbles, E.; Blacher, S.; Vanlathem, E.; Jerome, R.; Deltour, R.; Brouers, F.; Teyssle, P. Macromolescules 1995, 28, 1559.
11. Kohler, F. U.S. Pat. 3,243,753 (1966).
12. Meyer, J. Polym Eng Sci 1974, 14, 706.
13. Ohe, K.; Natio, Y. Jpn J Appl Phys 1971, 10, 99.
14. Sherman, R. D.; Middleman, L. M.; Jacobsa, S. M. Polym Eng Sci 1983, 23, 36.
15. Sumita, M.; Sakata, K.; Asai, S.; Miyasaka, K.; Nakagawa, H. Polym Bull 1991, 25, 265.
16. Reghu, M.; Yoon, C.; Yang, C.; Moses, D.; Heeger, A.; Cao, Y. Macromolecules 1993, 26, 7245.
17. Gubbles, F.; Jerome, R.; Teyssie, P.; Vanlathem, E.; Deltour, R.; Calderone, A.; Parente, V.; Bredas, J. Macromolecules 1994, 27, 1972.
18. Knackstedt, M. A.; Roberts, A. P. Macromolecules 1996, 29, 1369.
19. Keith, H. D.; Padden, F. J., Jr.; Russel, T. P. Macromolecules 1989, 22, 666.
20. Lee, J.-C.; Nakajima, K.; Ikehara, T.; Nishi, T. J Appl Polym Sci 1997, 65, 409.
21. Lee, J.-C.; Ikehara, T.; Nishi, T. J Appl Polym Sci 1998, 69, 193.
22. Ozin, G. A. Adv Mater 1992, 4, 612.
23. Novak, B. M. Adv Mater 1993, 5, 422.
24. Kojima, Y.; Usuki, A.; Kawasumi, M.; Okada, A.; Kurauchi, T.; Kamigaito, O.; Kaji, K. J Polym Sci Part B: Polym Phys 1988, 26, 1947.
25. Hulteen, J. C.; Martin, C. R. J Mater Chem 1997, 7, 1075.